

Electrochemical and Thermo Dynamical Investigation of 5-ethyl 4-(4-methoxyphenyl)-6-methyl-2-thioxo-1, 2, 3, 4 tetrahydropyrimidine-5-carboxylate on Corrosion Inhibition Behavior of Aluminium in 1M Hydrochloric Acid Medium

Rishi Korde¹, Chandra Bhan Verma¹, E.E. Ebenso², M.A. Quraishi^{1,*}

¹Department of Chemistry, Indian Institute of Technology, Banaras Hindu University, Varanasi-221005, India

²Material Science Innovation & Modelling (MaSIM) Research Focus Area, Faculty of Agriculture, Science and Technology, North-West University (Mafikeng Campus), Private Bag X2046, Mmabatho 2735, South Africa

*E-mail: maquraishi.apc@itbhu.ac.in, maquraishi@rediffmail.com

Received: 15 October 2014 / Accepted: 29 November 2014 / Published: 16 December 2014

Present investigation, describe the synthesis of 5-ethyl 4-(4-methoxyphenyl)-6-methyl-2-thioxo-1,2,3,4-tetrahydropyrimidine-5-carboxylate (INH) and its corrosion inhibition property on aluminium in 1M HCl using weight loss, potentiodynamic polarization and surface study methods. Tafel polarization measurements revealed that investigated inhibitor acts as mixed-type. The inhibitor exhibited the best inhibition efficiency of 83.33% at 500 ppm concentration. Adsorption of the inhibitor on aluminium surface in 1M HCl follows the Langmuir adsorption isotherm. Scanning electron microscopy (SEM) and dispersive X-ray spectroscopy (EDX) examinations was performed on inhibited and uninhibited aluminium samples to show the presence of inhibitor on aluminium surface. Some kinetic and thermodynamic parameters were also calculated to explain the nature and mechanism of adsorption.

Keywords: Acid corrosion, Aluminium, Thermodynamic parameter, potentiodynamic polarization

1. INTRODUCTION

Aluminium is extensively used in various industrial operations because of its corrosion resistance nature which is due to presence of surface oxide layer. However, during acid pickling aluminium undergoes sever corrosion and dissolution of surface oxide layer. Because of their practical usefulness, the development of corrosion inhibitors based on organic compounds has much scope in

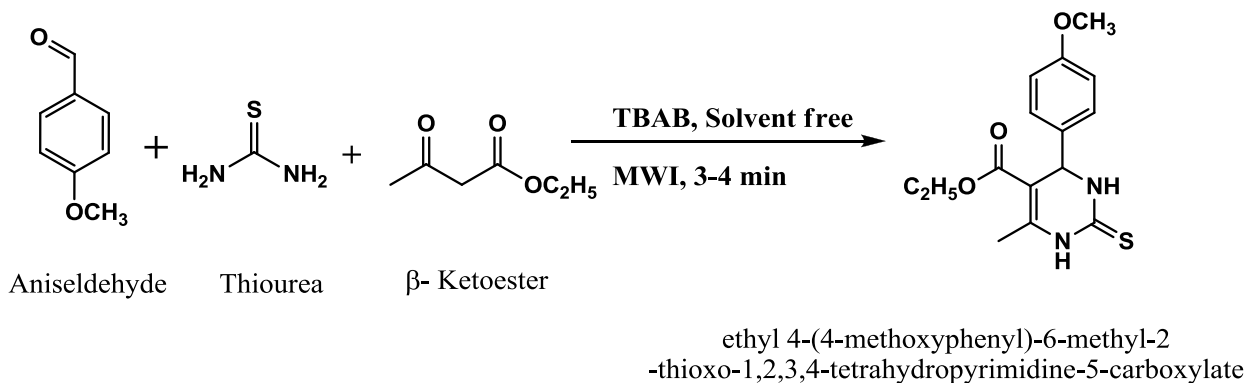
several industries. The molecular structure of organic compounds used as corrosion inhibitor has been found to exert a major influence on the extent of corrosion inhibition [1-4]. Aluminium and its alloys are widely used materials for their excellent electrical and thermal conductivities in many applications and recently in the manufacture of integrated circuits [5-6]. The chemical dissolution and electro plating are the main processes used in the fabrication of electronic devices. The most widely used pickling acid is HCl, so this medium has induced a great deal of research on Aluminium [11-17]. Most of the effective organic inhibitors have hetero atom such as O, N, S along with multiple bonds in their molecules through which they can adsorb on the metal surface.

In the present study we have synthesized 5-ethyl 4-(4-methoxyphenyl)-6-methyl-2-thioxo-1, 2, 3, 4-tetrahydropyrimidine-5-carboxylate and investigates its corrosion inhibition properties on aluminum in 1M HCl. The study was performed using weight loss measurement, potentiodynamic polarization, and surface investigation methods. The microwave irradiation has gained a powerful rapid tool for transformation of varieties of compounds including etherification, hydrolysis, etherification, addition, and rearrangement [18]. The application of microwave irradiation has several advantages over convention synthesis such as: uniform heating occurs throughout the material, reaction rate is increased, high reaction yield, higher atom economy, higher purity of product, improve reproducibility, environmental heat loss can be reduced, reduce wastage of heating reaction vessel and low operating cost [19].

2. EXPERIMENTAL SECTION

2.1 Inhibitors synthesis

The inhibitor used under present study was synthesized by ultrasound irradiation according to the Scheme 1 with slightly modified method as describe earlier in literature [20]. The reaction mixture was irradiated by ultrasound radiation for 3-4 min. The progress and completion of reaction was determined by TLC method using silica TLC plate prepared on aluminium plate. The product was catheterized by determination of melting point, FT-IR spectroscopy and ^1H NMR spectroscopic techniques. The melting point of the investigated compounds was determined using open capillary method. The characterization data of investigated compound is as follow: 5-ethyl 4-(4-methoxyphenyl)-6-methyl-2-thioxo-1,2,3,4-tetrahydropyrimidine-5-carboxylate M.P: 151–152°C; IR–(KBr): ν_{max} = 3252, 1657, 1585, 1569 cm^{-1} ; ^1H NMR (300 MHz), CDCl_3d_6 solution: δ 9.83 (br. s, 1H), 9.23 (br. s, 1H), 7.29 (d, J = 8.21 Hz, 2H), 6.23 (d, J = 8.1 Hz, 2H), 5.25 (s, 1H), 4.06 (q, J = 7.1 Hz, 2H), 2.28 (s, 3H), 1.18 (t, J = 7.2 Hz, 3H).



Scheme 1. Synthetic rout of investigated inhibitor.

2.2 Materials

The chemical, electrochemical measurements and surface studies were performed on aluminium species having grade Al-1060. All the weight loss experiments were performed on the aluminium specimens having exposed area $2.5 \times 2 \times 0.025 \text{ cm}^3$. The electrochemical experiments were performed on $7.5 \times 1 \times 0.025 \text{ cm}^3$ dimensions aluminum strip with exposed area of $1.0 \times 1.0 \text{ cm}^2$ and rest of the portion were covered with epoxy resin. Before the measurements performed the aluminium surface were cleaned with SiC abrasive papers of grades 600, 800, 1000, and 1200, respectively. Finally they were washed with acetone, dried and stored in moisture-free desiccators.

2.3 Test Solution

The test solutions of inhibitor was prepared by dissolving 3,4-dihydropyrimidine-2(1*H*)-ones/-thiones in 1M HCl and for dilution double distilled water was used.

2.4. Weight loss method

The weight loss measurements were performed on polished and degreased aluminium specimens for 3 h immersion time in 1M HCl which have exposed area $2.5 \times 2 \times 0.025 \text{ cm}^3$. After completion of 3h the aluminium specimens were taken out washed with double distilled water, dried and weight accurately. The calculation of the inhibition efficiency (η %) and surface coverage (θ) was carried out using the following equations:

$$\eta\% = \frac{C_R - C_{R(i)}}{C_R} \times 100 \quad (1)$$

$$\theta = \frac{C_R - C_{R(i)}}{C_R} \quad (2)$$

where, C_R and $C_{R(i)}$ are the corrosion rate values in absence and presence of inhibitor, respectively. The corrosion rate (C_R) of aluminium in acidic medium was calculated by using following equation:

$$C_R = \frac{W}{At} \quad (3)$$

where, W is weight loss of aluminium specimens (mg), A is the area of the specimen (cm^2) and t is the exposure time (h).

2.5. Potentiodynamic polarization measurements

The potentiodynamic polarization measurements were performed on aluminium specimens in 1M HCl using Potentiostat / Galvanostat (model G-300) connected with a personal computer consisting of EIS software (Gamry Instruments Inc., USA) controlled by Gamry Echem Analyst 5.0 software. The Potentiostat / Galvanostat consist of conventional three electrode assembly in which the aluminium specimens with exposed area 1cm^2 was used as working electrode, the high purity platinum foil (1cm^2) was used as counter electrode and the saturated calomel electrode was used as reference electrode. The three electrode assembly allowed to stand for 30 min in order to stabilize open circuit potential (E_{OCP}) i.e. the potential develop on aluminium surface without applying any potential. All the potentiodynamic polarization measurements were performed by automatically changing the electrode potential from -250 to $+250$ mV vs. corrosion potential saturated calomel electrode (SCE) at the scan rate of 1mVs^{-1} . The potentiodynamic nature of aluminium in 1M HCl was studied by recording the cathodic and anodic Tafel curves in absence and presence of different concentration of inhibitors. The corrosion current densities were determined with and without inhibitor by extrapolating the anodic and cathodic curves to corrosion potential. From calculated corrosion current densities corrosion inhibition efficiency was determined using following equation:

$$\eta\% = \frac{i_{\text{corr}}^0 - i_{\text{corr}}^i}{i_{\text{corr}}^0} \times 100 \quad (4)$$

where i_{corr}^0 and i_{corr}^i are the corrosion current densities in the absence and presence of investigated inhibitor, respectively.

3. RESULTS AND DISCUSSIONS

3.1 Weight loss studies

3.1.1 Effect of inhibitor concentration

The weight loss experiments were performed on aluminum surface in 1M HCl for 3 h immersion time. Variation of the inhibition efficiency with concentration is shown in Figure 1(a). Various weight loss parameters such as corrosion rate (C_R), surface coverage (θ) and corresponding inhibition efficiency (η %) were determined from the weight loss experiment are listed in Table

1.From Figure 1 (a) and results depicted into Table 1 it is observed that inhibition efficiency of the inhibitor under present study increases with increasing concentration. This increase in the inhibition efficiency and surface coverage is due to increase in adsorption of inhibitor molecule on increasing concentration.

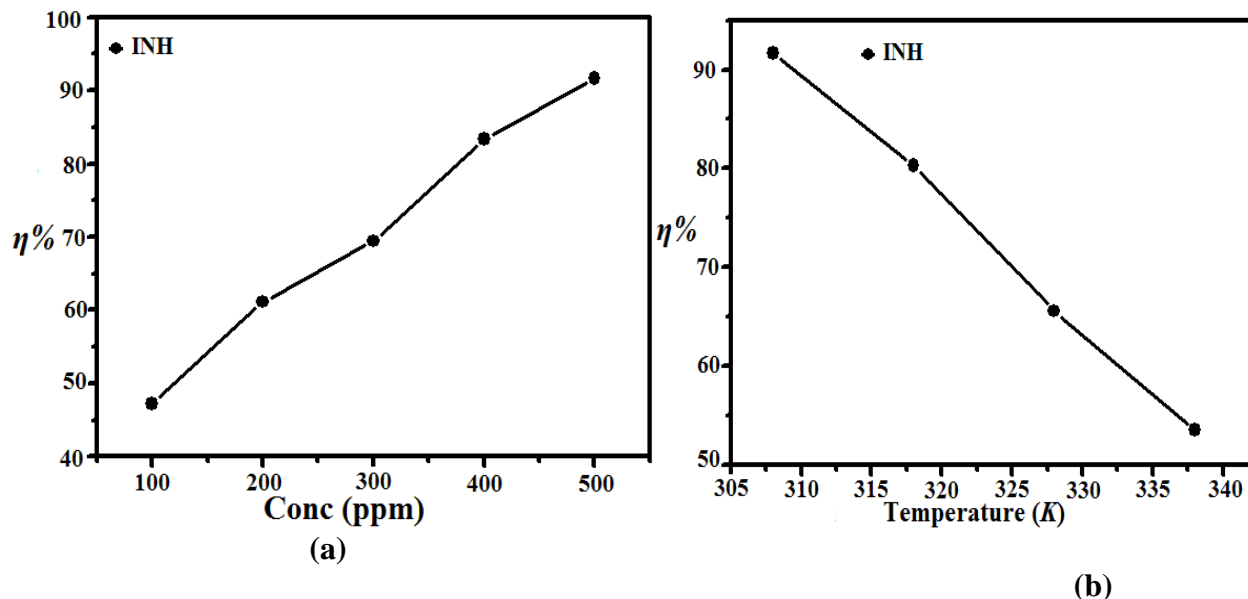


Figure 1 (a, b). (a) Inhibition efficiency of inhibitor at different concentration (b) Inhibition efficiency of inhibitor at different temperature

3.1.2. Effect of Temperature

The weight loss experiments were also performed on aluminium specimens in temperature range of 308 – 338 K to investigate the effect of temperature on corrosion. The variation of inhibition efficiency with temperature is depicted in Figure 1(b). Inspection of the Figure 1 (b) revealed that inhibition efficiency decreases and corrosion rates increases on increasing temperature. This decrease in inhibition performance of inhibitor is due to desorption of the adsorb inhibitor molecules at elevated temperature from aluminium surface [21]. Therefore, more desorption takes place on increasing temperature resulting into larger area of aluminium come into contact of acid solution resulting in an increase in corrosion rate at elevated temperature.

Table 1. Corrosion rate (C_R), Surface coverage (θ) and inhibition ($\eta\%$) for aluminium in 1N HCl in absence and in presence of different concentrations of inhibitor from weight loss measurements at 308 K.

Inhibitor	Conc (ppm)	Weight loss(mg)	Surface coverage(θ)	Inhibition efficiency($\eta\%$)	Corrosion rate($\text{mg cm}^{-2} \text{h}^{-1}$)
Blank	-	36	-	-	1.2

Inhibitor	100	19	0.4722	47.22	0.6333
	200	14	0.6111	61.11	0.4667
	300	11	0.6944	69.44	0.3667
	400	6	0.8333	83.33	0.2
	500	3	0.9166	91.66	0.1

3.1.3 Thermodynamically parameters and Adsorption isotherms:

The corrosion inhibition of aluminium in 1M HCl can be best explained in term of molecular adsorption of inhibitor on its surface [22]. To describe the adsorption behavior of inhibitor on aluminium surface, several adsorption isotherms were tested including Temkin, Frumkin and Langmuir adsorption isotherms. Out of various adsorption isotherms Langmuir isotherm give best fit which is plotted between $\log(\theta/1-\theta)$ and $\log C$ [Figure 2 (a)], with a regression coefficient very close to unity which validate the fitness of the Langmuir adsorption isotherm. The Langmuir isotherm is generally represented by following formula [22]:

$$\frac{C_{(inh)}}{\theta} = \frac{1}{K_{(ads)}} + C_{(inh)} \tag{5}$$

where, $C_{(inh)}$ is the concentration of inhibitor and K_{ads} is the constant for adsorption and desorption processes occurring on aluminium surface. The value of K_{ads} related to the free energy of adsorption (ΔG°_{ads}) as following formula [23]:

$$\Delta G^{\circ}_{ads} = -RT \ln(55.5K_{ads}) \tag{6}$$

The value of ΔG°_{ads} and K_{ads} were calculated using above formula at different temperature and given in Table 2. The significant negative values of ΔG°_{ads} suggest that adsorption of inhibitor on aluminium surface is a strong and spontaneous process [24].

Table 2. The values of K_{ads} and ΔG°_{ads} for aluminium in absence and presence of different concentration of inhibitor in 1M HCl at different temperature.

inhibitor	$K_{ads} (10^3 M^{-1})$				$-\Delta G^{\circ}_{ads} (kJ mol^{-1})$			
	308	318	328	338	308	318	328	338
INH	13.6	6.49	4.04	1.79	34.68	33.83	33.60	32.34

Generally, the value of ΔG°_{ads} is more than $-20 kJmol^{-1}$ related to electrostatic attraction between inhibitor and metal surface i.e. physical adsorption and less than $-40 kJmol^{-1}$ is related to the charge sharing between inhibitor and metal i.e. chemical adsorption [25,26]. However, in our present case values of ΔG°_{ads} ranges in between -32.34 to -34.68 suggesting that adsorption of the inhibitor on aluminum surface follow the physical as well as chemical mode of adsorption predominantly chemical adsorption [27].

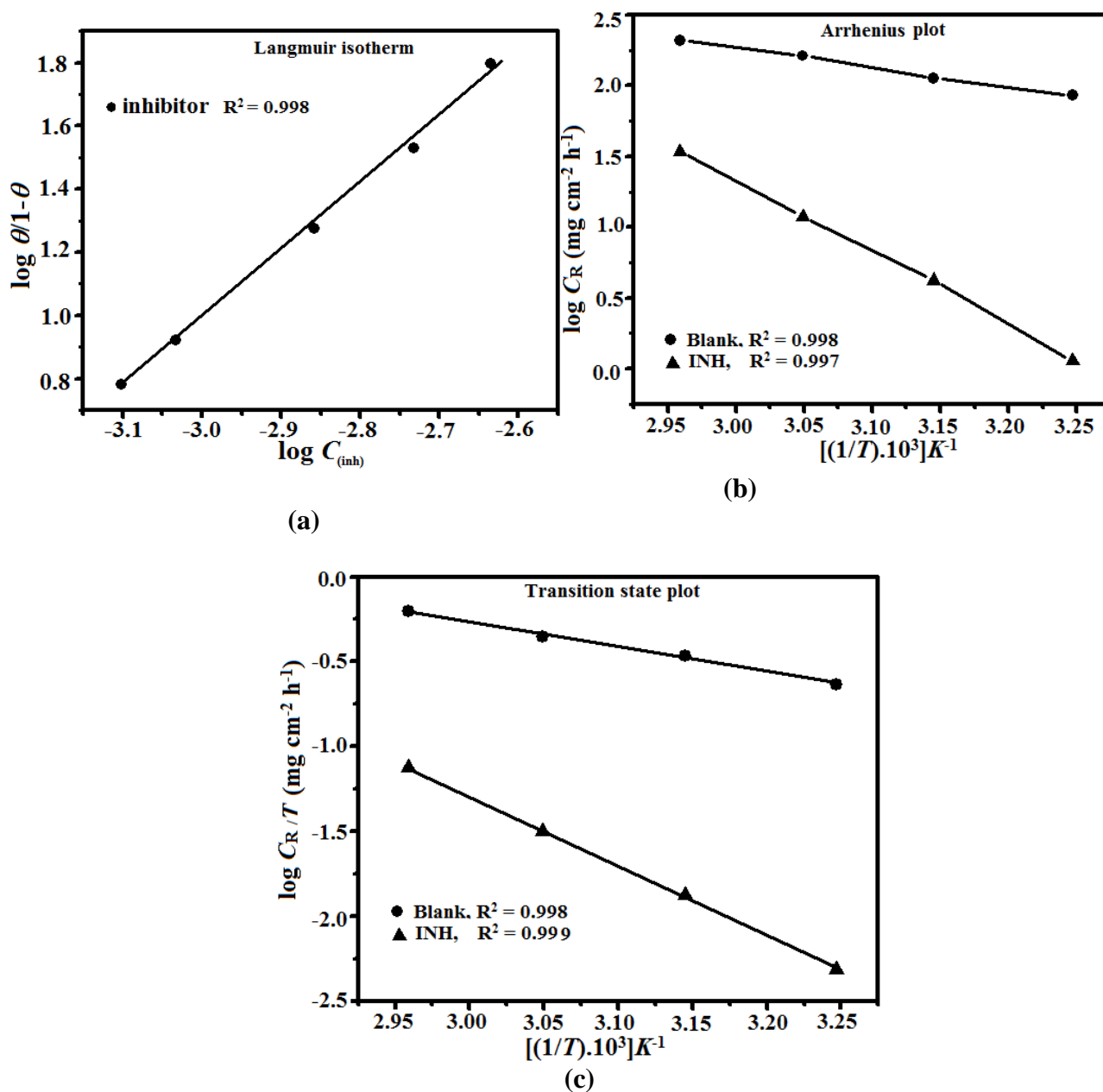


Figure 2. (a) Langmuir adsorption isotherm (b) Arrhenius plot of $\log C_R$ vs. $1/T$ (c) Transition state plot of $\log C_R/T$ vs. $1/T$

The value of apparent activation energy (E_a) was calculated from Arrhenius equation:

$$\log(C_R) = \frac{-E_a}{2.303RT} + \log \lambda \tag{7}$$

where, E_a is the apparent activation energy (J mol^{-1}), R is the molar gas constant ($8.314 \text{ J K}^{-1} \text{ mol}^{-1}$), T is the absolute temperature (K), and λ is the Arrhenius pre-exponential factor. The Arrhenius plot gives a straight line between $\log C_R$ vs $1/T$ as shown in Figure 2 (b). The E_a values were calculated by multiplying the slope of Arrhenius plots ($\log C_R$ vs $1/T$) by $2.303R$ and represented in Table 3. From the Table 3 it is depicted that activation energies is greater (97.52 kJmol^{-1}) in presence of inhibitor than in its absence (24.41 kJmol^{-1}). The larger value of E_a in presence of the inhibitor

suggests that aluminium dissolution in 1M HCl is mainly controlled by increasing the activation energy barriers for corrosion process [28, 29].

The corrosion rate dependency on temperature can also be represented by transition state equation:

$$C_R = \frac{RT}{Nh} \exp\left(\frac{\Delta S^*}{R}\right) \exp\left(-\frac{\Delta H^*}{RT}\right) \quad (8)$$

where, ΔH^* is the apparent enthalpy of activation, ΔS^* the apparent entropy of activation, h is Planck's constant and N is the Avogadro number. The transition state plot [Figure 2 (c)] give a straight line between $\log C_R/T$ vs $1/T$. in Table 3 from the slope of $(-\Delta H^*/2.303R)$ and intercept of $[\log(R/Nh) + (\Delta S^*/2.303R)]$ values ΔS^* and ΔH^* were calculated and listed in Table 3. From the Table 3 it is clear that ΔH^* in presence of inhibitor is larger (78.87kJ mol^{-1}) than in free 1M HCl solution (19.39kJ mol^{-1}). The positive sign and higher value of ΔH^* reflects the endothermic nature of aluminium dissolution process, meaning that dissolution of aluminium is difficult in presence of inhibitor [30].

Table 3. Activation parameters for aluminium dissolution in 1M HCl in the absence and presence of different concentration of investigated inhibitor

inhibitor	E_a	ΔH^*	ΔS^*
Blank	24.41	19.39	-152.9
INH	97.52	78.87	14.18

Inspection of the Table 3 reveals that values of entropies (ΔS^*) are higher $14.18\text{kJ}^{-1}\text{mol}^{-1}$) in presence of inhibitor than in absence ($152.9\text{kJ}^{-1}\text{mol}^{-1}$) suggesting the formation of activated complex in the rate determining step represents dissociation rather than association, meaning that disordering increases on going from reactants to the activated complex [31].

3.2 Potentiodynamic polarization measurements:

To investigate the effect of inhibitor on the anodic and cathodic reaction of aluminum in 1M HCl, the Tafel polarization study was performed at different concentration of the inhibitor. Typical potentiodynamic polarization curves were observed for aluminium in 1N HCl in absence and presence of different concentration of inhibitor as shown in Figure 3. The potentiodynamic polarization parameters derived from the Tafel polarization curves are given in Table 4. The corrosion current densities were calculated by extrapolating the cathodic and anodic Tafel slopes to corrosion potential. The study of Table 4 reveals that addition of the inhibitor seems to affect anodic as well as cathodic partial reaction.

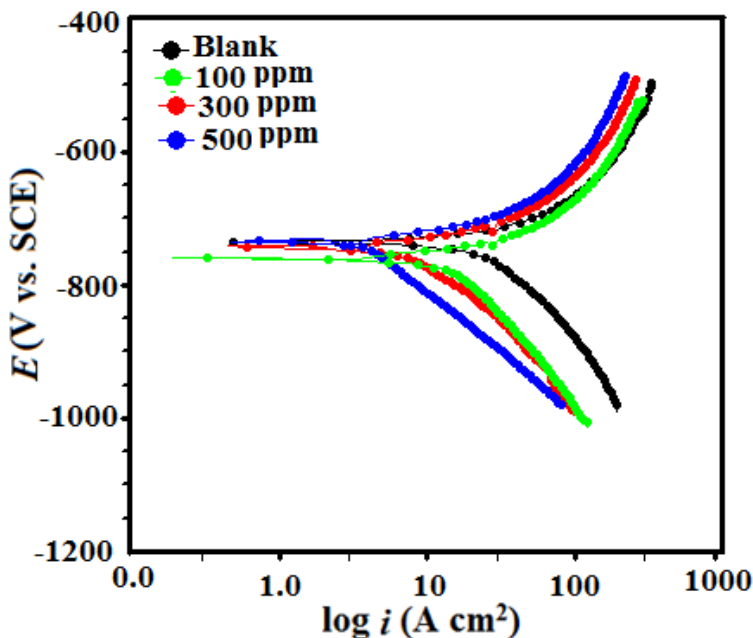


Figure 3. Tafel polarization curves for corrosion of aluminium in 1M HCl in the absence and presence of different concentrations inhibitor

The inhibitor can be classified into anodic, cathodic or mixed type depending upon the value of E_{corr} . If the value of E_{corr} in presence of inhibitor is > 85 mV vs SCE compare to free acid solution, the inhibitor can be classified into anodic or cathodic type, however, when the values of E_{corr} is less in presence of inhibitor than the value E_{corr} in absence of inhibitor, the inhibitor can be classified as mixed type [32]. In our present investigation the corrosion potential (E_{corr}) value shifted slightly this indicates that all the studied inhibitor acted as mixed type inhibitor in 1N HCl [25-28]. The decrease in i_{corr} value indicates the adsorption of inhibitor molecules on metal surfaces [33].

Table 4. The Electrochemical parameters and corresponding efficiencies of inhibitor in 1 N HCl at different concentration of inhibitor

Tafel data							
Inhibitor	Conc ppm	i_{corr} (mA/cm ²)	E_{corr} (mV/SCE)	β_a (mV/dec)	β_c (V/dec)	θ	$\eta\%$
Blank	0.0	91.20	-735.0	184.3	1.000e15
Inhibitor	100	43.50	-759.0	132.6	1.000e15	0.5230	52.30
	300	21.30	-742.0	101.0	1.132e15	0.7665	76.65
	500	6.030	-733.0	41.60	1.247e15	0.9339	93.39

3.3 Surface Study

3.3.1 Scanning Electron microscopic (SEM) analysis

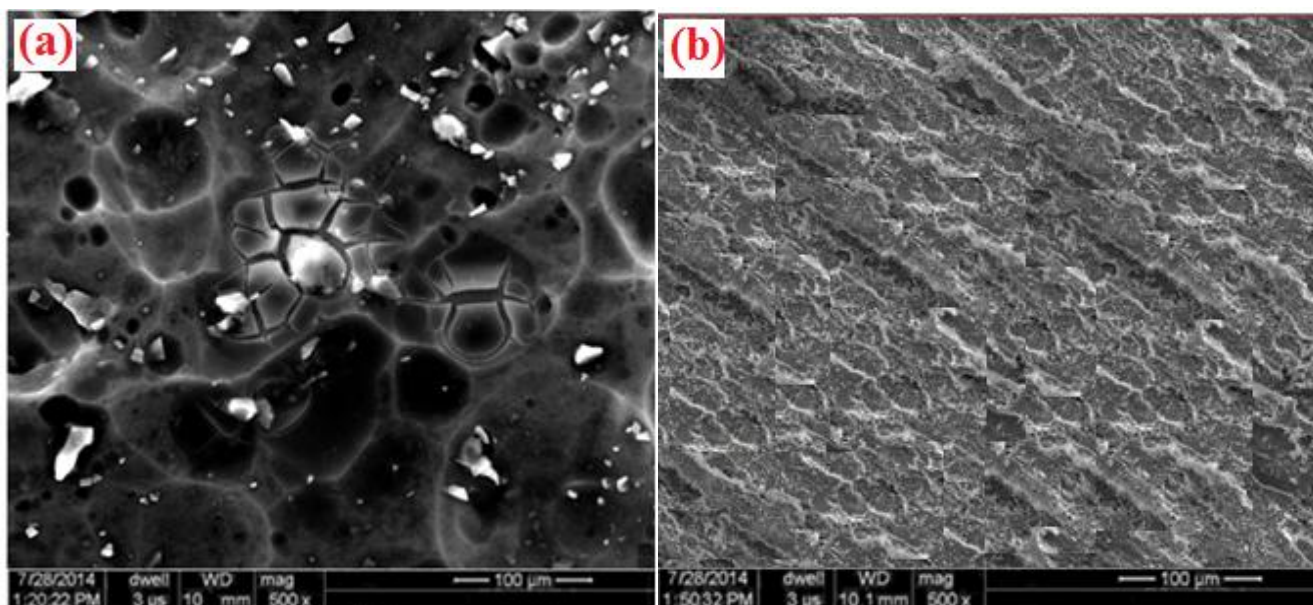


Figure 4. SEM micrographs of aluminium surfaces: (a) uninhibited 1M HCl, and in the presence of (b) inhibitor

The SEM measurements were performed on aluminium surface in absence and presence of optimum concentration of inhibitor after 3h immersion time using a SEM model FEI Quanta 200F microscope at 500× magnification. Figure 4 (a-b), represent the SEM micrograph of aluminum in absence and presence of optimum concentration of inhibitor. The aluminium surface in absence of inhibitors [Figure 4 (a)] is characterized by highly corroded surface with pits and cracks which is due to free acid corrosion of the aluminium surface in 1M HCl. However, in presence of inhibitor [Figure 4 (b)] the aluminium surface morphology is remarkably improved due formation of protective film of inhibitor which protect the aluminium surface from corrosion.

3.3.2 X-ray spectroscopy (EDX) measurements

Similar to SEM, EDX analysis were also performed on aluminium surface in 1M HCl with and without inhibitor for 3h immersion time to show the presence of inhibitor on metal surface. Figure 5 (a) represents the EDX micrograph of aluminium in 1M HCl without inhibitor which is characterized by a characteristic peak for aluminium. The peaks for nitrogen (N), Oxygen (O) and Sulfur (S) were absent. However, the EDX spectra in presence of inhibitor [Figure 5 (b)] show a characteristic signal for N, O and S suggesting that inhibitor form a protective film on aluminium surface and protect it from free acid corrosion.

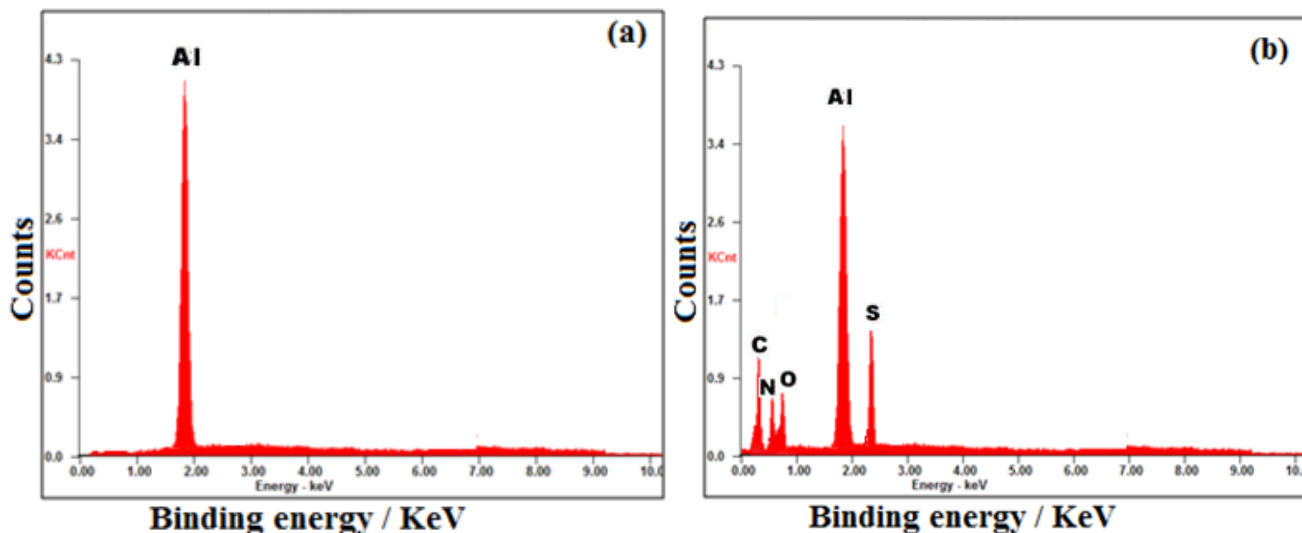


Figure 5. EDX spectra of aluminum in (a) absence of inhibitor (b) in presence of inhibitor

4. MECHANISM OF INHIBITION

From the potentiodynamic polarization, weight loss and surface measurements it can be concluded that inhibitor inhibits aluminium corrosion in 1M HCl by adsorption process. The adsorption of the inhibitor on metal surface depend upon various factors including presence of substituents, nature of electron donating and electron withdrawing groups and type of corrosive medium. Organic molecules may be adsorbed on the metal surface in four ways namely [34-36],

- (i) Electrostatic interaction between the charged molecules and the charged metal,
- (ii) Interaction of unshared electron pairs in the molecule with the metal,
- (iii) Interaction of π -electrons with the metal

In acid solution, inhibitor molecules bear's positive charge due to protonation of the heteroatoms present in inhibitor. The heteroatoms are easily protonated in acid solution due to presence of lone pair of electron. Moreover, the aluminum surface bear's negative charge in acid solution due to presence of surface chloride ions [37]. The negatively charged inhibitor molecules attracted the positively charged inhibitor by electrostatic attraction (physisorption). As soon as inhibitor come in contact with aluminium surface it abstract the electron from metal and release H_2 gas and come its neutral form. The neutral from of inhibitor donate its lone pair of electron to the empty orbital of the metal and adsorb chemically (chemisorption). However, accumulation of the negative charge on metal surface renders it to release the electrons into anti bonding molecular orbital of the inhibitor by retro donation [38]. Thus it can be concluded that greater the electron donation from the inhibitor to metal, greater will be retro donation. The various mode of interaction of inhibitor in aluminium surface in 1 M HCl is shown in Figure 6.

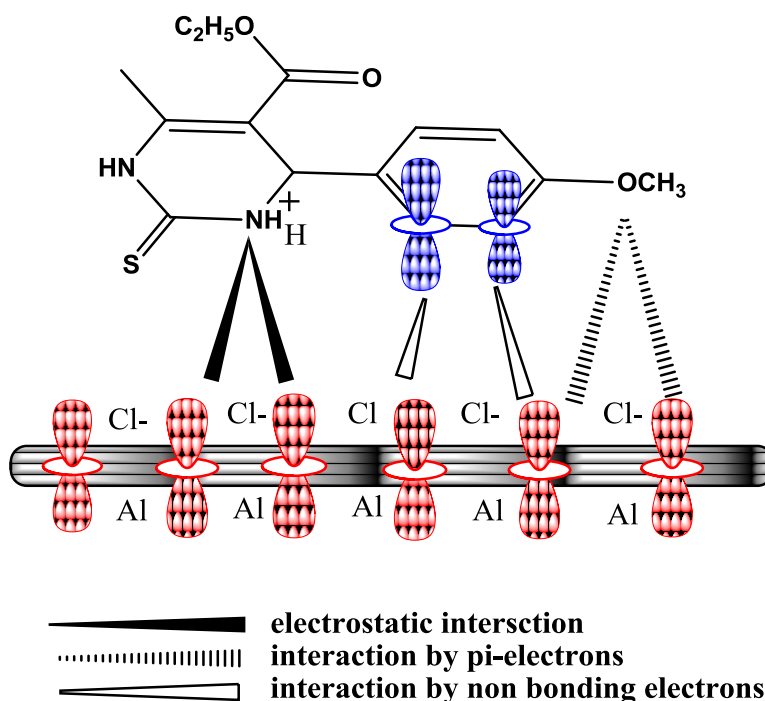


Figure 6. Pictorial presentation of various force acting between metal surface and inhibitor molecule

5. CONCLUSIONS

1. The 5-ethyl 4-(4-methoxyphenyl)-6-methyl-2-thioxo-1, 2, 3, 4-tetrahydropyrimidine-5-carboxylate are good corrosion inhibitors for aluminium in 1N HCl solution.
2. The inhibition efficiencies increase with increasing concentration and maximum efficiency was obtained at 500 ppm concentration.
3. The potentiodynamic polarization study revealed that investigated inhibitor behaves like a mixed-type inhibitor.
4. The adsorption of the inhibitor on aluminium surface in 1 M HCl follows the Langmuir adsorption isotherm.
5. The large negative value of the free energy of adsorption suggest that adsorption of the investigated inhibitor on aluminium in 1M HCl is a spontaneous process.
6. The inhibition efficiencies obtained from polarization measurements data are comparable with those obtained from Gravimetric data.

Reference

1. J.W. Diggle, T.C. Downie, C.W. Goulding, *Chem. Rev.*, 65 (1969) 365.
2. C.M.A. Brett, *J. Appl. Electrochem.*, 20 (1990) 1000.
3. J.B. Bessone, D.R. Salinas, C.E. Mayer, W.J. Lorenz, *Electrochim. Acta.*, 37 (1992) 2283.
4. G.R.T. Schueller, S.R. Taylor, E.E. Hajcsar, *J. Electrochem. Soc.*, 139 (1992) 2799.
5. T.D. Burleigh, A.T. Smith, *J. Electrochem. Soc.*, 139 (1992) 2799.

6. E.J. Lee, S.J. Pyun, *Corros. Sci.*, 37 (1995) 157.
7. A. Frichet, P. Gimenez, M. Keddam, *Electrochim. Acta.*, 38 (1996) 1957.
8. W. Linderink, M.V.D. Linden, J.H.W. Wit, *Corros. Sci.*, 38 (1993) 1989.
9. T.R. Beck, *Electrochim. Acta.*, 33 (1988) 1321.
10. G. Brett, *Electrochim. Acta.*, 33 (1988) 1321.
11. F.D. Bogar, R.T. Foley, *J. Electrochem. Soc.*, 119, (1972) 462.
12. S. Szklarska-Smialowska, *Corros. Sci.*, 33 (1992) 1193.
13. Olesegun K.Abiola, J.O.E.Otaigbe, O.J.Kio, *Corros. Science.*, 51 (2009) 2790.
14. I.B.Obot, N.O.Obi – Egbedi, Portugaliae *Electrochemical Acta.*, 27 (2009) 517.
15. Enteram A.Noor, *J.Appl.Electrochem.*, 39 (2009) 1465.
16. Olesegun K. Abiola, J.O.E. Otaigbe, O.J.Kio., *Corros. Sci.*, 51 (2009) 1879.
17. M. Shyamala, A. Arulanantham, *NEPT* 7 (2008) 415.
18. P. Lindstrom, J.Tierney, B. Wathey, J. Westman, *Tetrahedron.*, 57 (2001) 9225.
19. C.B. Verma, M. J. Reddy, M. A. Quraishi, *Anal. Bioanal. Electrochem.*, 6 (2014) 515.
20. M.Vijey Aanandhi, R.Kamal Raja, G.Devdassa, R.Sujathab, P.Shanmugasundaram, *Rasayan J. Chem* 3 (2008) 586.
21. Sudheer, M.A. Quraishi, *Corros. Sci.* 70 (2010) 161.
22. I. Ahamad. R. Prasad and M.A. Quraishi. *Corros. Sci.* 52 (2010) 1472
23. M. J. Reddy, C. B. Verma, E.E Ebenso, K. K. Singh, M. A. Quaraishi, *Int. J. Electrochem. Sci.*, 9 (2014) 4884.
24. M. A. Quraishi, I. Ahamad, A. K. Singh, S. K. Shukla, B. Lal, V. Singh, *Mater. Chem. Phys.* 2008, 112, 1035–1039
25. L. Li, X. Zhang, J. Lei, J. He, S. Zhang, F. Pan, *Corros. Sci.* 63 (2012) 82.
26. A. O. Yüce, G. Kardaş, *Corros. Sci.* 58 (2012) 86.
27. Sudheer, M. A. Quraishi, *Ind. Eng. Chem. Res.* 5320 (14) 2851.
28. C.B. Verma, M.A. Quraishi, E.E. Ebenso. *Int. J. Electrochem. Sci.*, 8 (2013) 7401
29. L. Larabi, Y. Harek, O. Benali, S. Ghalem, *Prog. Org. Coat.* 54 (2005) 256.
30. N.M. Guan, L. Xueming, L. Fei, *Mater. Chem. Phys.* 86 (2004) 59–68.
31. M.A. Quraishi, A. Singh, V.K. Singh, D.K. Yadav, A.K. Singh, *Mater. Chem. Phys.*, 122 (2010) 114.
32. C. B. Verma, M. J. Reddy, M. A. Quraishi, *Anal. Bioanal. Electrochem.*, 6 (2014) 321
33. O. Riggs, L.Jr. Corrosion Inhibitors, 2nd ed.; C. C. Nathan (1973) Houston, TX, USA,; p 109
34. D.P. Schweinsberg, G.A. George, A.K. Nanayakkara, D.A. Steiner, *Corros. Sci.* 28 (1988)33.
35. H. Shorky, M. Yuasa, I. Sekine, R.M. Issa, H.Y. El-Baradie, G.K. Gomma, *Corros. Sci.* 40 (1998) 2173.
36. A.K. Singh, M.A. Quraishi, *Corros. Sci.* 52 (2010) 152.
37. C. B. Verma M.A. Quraishi, *IJIRSET.*, 3 (7) (2014) 14601
38. G.N. Mu, T.P. Zhao, M. Liu, T. Gu, *Corros.* 52 (1996) 853.